ARTICLE

OBC
www.rsc.org/obc

Crystallographic studies on the reaction of isopenicillin N synthase with an unsaturated substrate analogue

Jonathan M. Elkins, Peter J. Rutledge,† Nicolai I. Burzlaff,‡ Ian J. Clifton, Robert M. Adlington, Peter L. Roach§ and Jack E. Baldwin*

The Dyson Perrins Laboratory and the Oxford Centre for Molecular Sciences, University of Oxford, South Parks Road, Oxford, UK OX1 3QY.
E-mail: jack.baldwin@chem.ox.ac.uk

Received 16th December 2002, Accepted 5th March 2003
First published as an Advance Article on the web 21st March 2003

Isopenicillin N synthase (IPNS) catalyses conversion of the linear tripeptide δ-(L-α-aminoadipoyl)-L-cysteinyl-D-valine (ACV) to isopenicillin N (IPN), the central step in biosynthesis of the β-lactam antibiotics. The unsaturated substrate analogue δ-(L-α-aminoadipoyl)-L-cysteinyl-D-vinylglycine (ACvG) has previously been incubated with IPNS and a single product was isolated, a 2-α-hydroxymethyl isopenicillin N (HMPen), formed *via* a monooxygenase mode of reactivity. ACvG has now been crystallised with IPNS and the structure of the anaerobic IPNS:Fe(II):ACvG complex determined to 1.15 Å resolution. Furthermore, by exposing the anaerobically grown crystals to high-pressure oxygen gas, a structure corresponding to the bicyclic product HMPen has been obtained at 1.60 Å resolution. In light of these and other IPNS structures, and recent developments with related dioxygenases, the [2 + 2] cycloaddition mechanism for HMPen formation from ACvG has been revised, and a stepwise radical mechanism is proposed. This revised mechanism remains consistent with the observed stereospecificity of the transformation, but fits better with apparent constraints on the coordination geometry around the active site iron atom.

Introduction

Isopenicillin N synthase (IPNS) catalyses conversion of the tripeptide δ-(L-α-aminoadipoyl)-L-cysteinyl-D-valine (ACV, **1**) to isopenicillin N (IPN, **2**), the central step in the biosynthesis of penicillin and cephalosporin antibiotics. IPNS is a non-haem iron(II)-dependent enzyme and utilises one equivalent of molecular oxygen in the bicyclisation reaction.[1] The bicyclisation is believed to proceed *via* initial β-lactam closure to give a monocyclic intermediate, associated with a high valent iron(IV)–oxo species (Fig. 1a), which then mediates closure of the five-membered thiazolidine.[2,3]

Solution-phase experiments with a wide range of substrate analogues have shown IPNS to exhibit broad substrate specificity, accepting a large number of modified tripeptides as substrates.[4] It is in the position of the valinyl residue that the enzyme has proved least discriminating. When IPNS was incubated with the unsaturated substrate analogue δ-(L-α-aminoadipoyl)-L-cysteinyl-D-vinylglycine (ACvG, **3**), a 2-α-hydroxymethyl penam (HMPen, **4**) was the only product isolated (Fig. 1b).[5] Labelling studies with several related unsaturated substrates have shown the incorporation of $^{18}O_2$ into other hydroxylated products,[6] and it is probable that this is also the case with HMPen **4**. Formation of the hydroxylated product **4** from ACvG was rationalised in terms of a monooxygenase (−2H, +O) pathway, with a mechanism involving a [$2\pi_s + 2\pi$] cycloaddition of the iron–oxene to the *re* face of the alkene (Fig. 1b).[6,7] Incubation of stereospecifically deuterium labelled isotopomers produced hydroxymethyl-penams in which the deuterium labels were not scrambled, supporting a stereospecific mechanism and consistent with the proposed cycloaddition.[8]

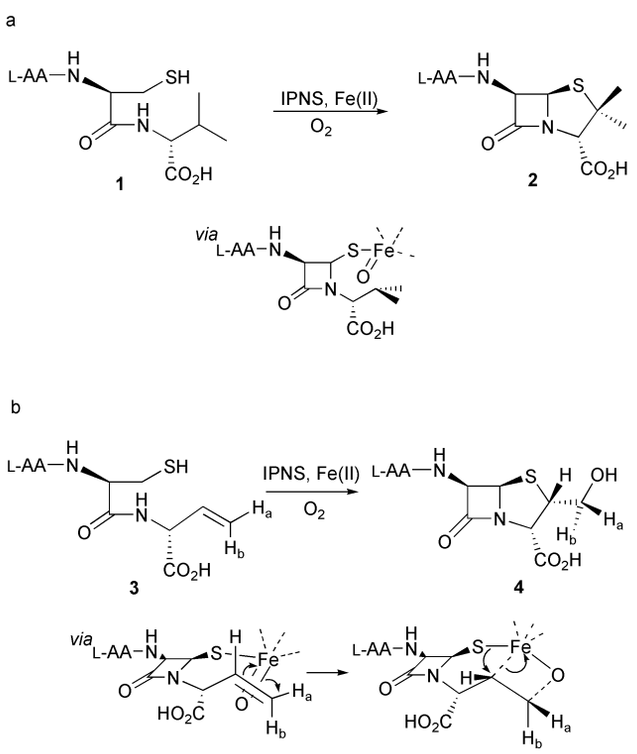

Fig. 1 The reaction of IPNS with **a**, its natural substrate ACV **1**; and **b**, the unsaturated analogue ACvG **3**, including an outline representation of the mechanism previously proposed for this reaction; L-AA = L-α-aminoadipoyl.

Recently, the application of pseudo-time-resolved crystallography to IPNS has allowed structural investigation of incubation results previously observed in solution. By subjecting IPNS:Fe(II):substrate crystals to high pressures of oxygen gas, crystals containing IPNS:Fe(II):product complexes can be obtained.[3,9,10] We have recently reported solution of a structure for the IPNS:Fe(II):IPN complex, obtained from high-pressure

† *Current address*: Department of Chemistry, University College Dublin, Belfield, Dublin 4, Ireland.
‡ *Current address*: Fachbereich Chemie, Universität Konstanz, 78457 Konstanz, Germany.
§ *Current address*: Department of Chemistry, University of Southampton, Highfield, Southampton, UK SO17 1BJ.

DOI: 10.1039/b212270g

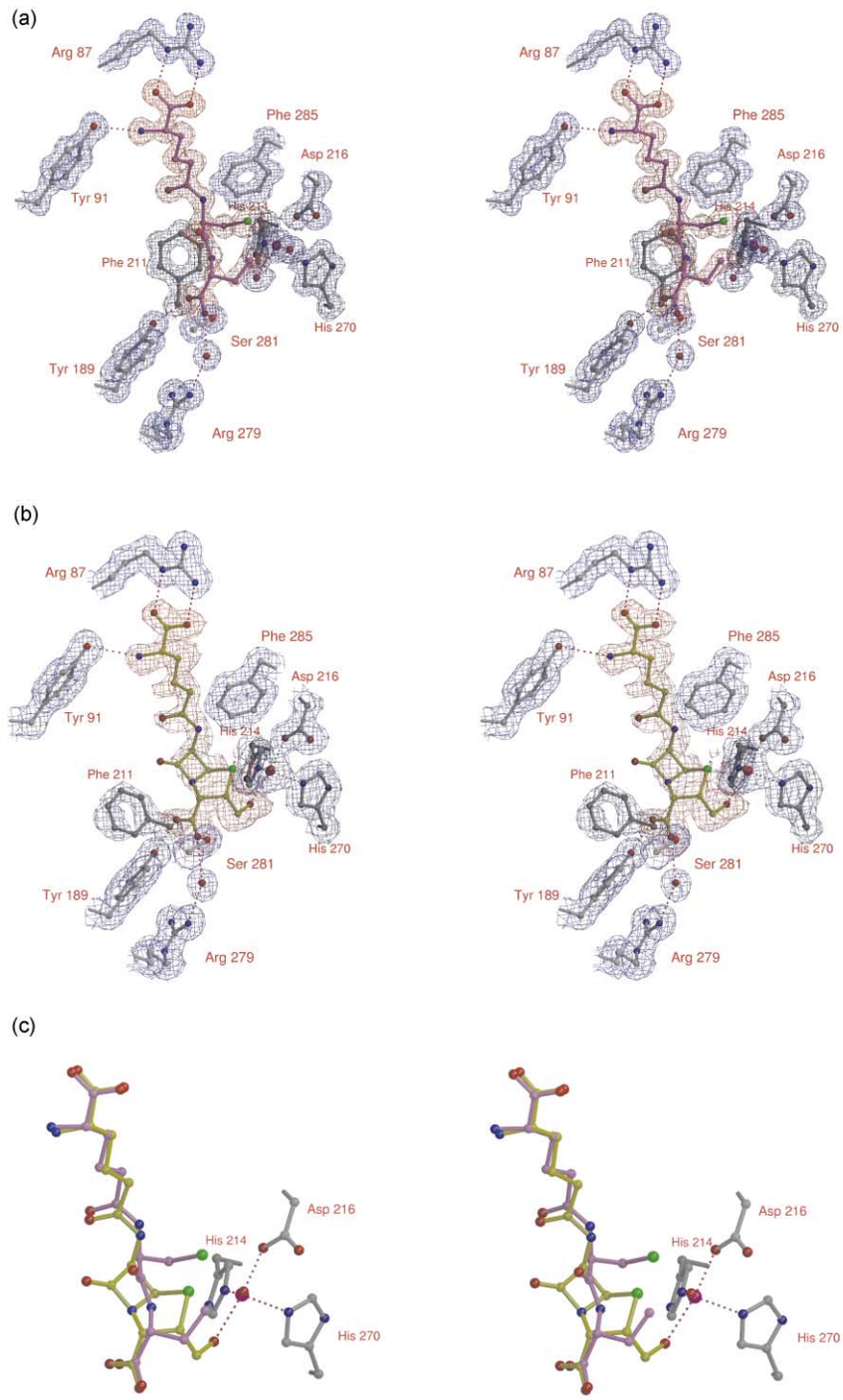

Fig. 2 Stereofigures showing IPNS in complex with ACvG and HMPen. **a**, The anaerobic IPNS:Fe(II):ACvG complex with a $2mF_o - DF_c$ electron density map contoured at 1σ around the protein atoms (in blue) and a $mF_o - DF_c$ omit map contoured at 3.2σ around ACvG (in red); **b**, the IPNS:Fe(II):HMPen complex with a $2mF_o - DF_c$ electron density map contoured at 1σ around the protein atoms (in blue) and a $mF_o - DF_c$ omit map contoured at 2.5σ around HMPen (in red); **c**, an overlay of the IPNS:Fe(II):ACvG and IPNS:Fe(II):HMPen structures to show the changes that have occurred in the course of reaction.

oxygenation of IPNS crystals incorporating iron and natural substrate ACV.[3] Attempts to obtain an enzyme:product complex in this manner were complicated by the release of product from the active site (N. I. Burzlaff, unpublished results). It was hypothesised that the hydroxymethyl penicillin **4** would be more firmly tethered to iron in the IPNS active site than the natural product IPN, by virtue of the additional hydroxyl ligand to the metal, and thus could allow improved structural characterisation of an IPNS:Fe(II):product complex.

Here we report the X-ray crystal structure of the IPNS:Fe(II):ACvG complex, and a structure for the IPNS:Fe(II):HMPen complex, obtained by high-pressure oxygenation of IPNS:Fe(II):ACvG crystals. These results, in combination with previous X-ray crystallographic studies,[3,11] allow proposal of a revised mechanism for the IPNS reaction cycle in its monooxygenase mode of reactivity.

Results and discussion

Structure of the IPNS:Fe(II):ACvG complex

The structure of the IPNS:Fe(II):ACvG complex was determined to 1.15 Å resolution (Fig. 2a). The overall structure of the protein is essentially identical to the IPNS:Fe(II):ACV structure.[11] The tripeptide substrate analogue also adopts a very similar conformation to that of the natural substrate, with only

Table 1 Data collection and statistics

Complex	IPNS:Fe(II):ACvG		IPNS:Fe(II):HMPen	
X-ray source	ID14-4 ESRF		Station 7.2 SRS	
Wavelength λ/Å	0.9312		1.488	
Space group	$P2_12_12_1$		$P2_12_12_1$	
Unit cell (*a*/Å, *b*/Å, *c*/Å)	46.401, 71.393, 100.906		46.534, 70.751, 100.876	
Resolution shell/Å	29.11–1.15	1.21–1.15	41.17–1.60	169–1.60
Measurements	375623	23648	101990	14387
Unique reflections	115554	13622	42669	6077
Multiplicity	3.3	1.7	2.4	2.4
Average $I/\sigma(I)$	6.2	5.3	6.4	1.9
Completeness (%)	96.2	78.9	95.2	94.2
R_{merge} (%)[a]	6.1	11.9	7.4	33.8
R_{cryst} (%)[b]	14.3		15.1	
R_{free} (%)[c]	15.2		17.8	
RMS deviation[d]	0.007 Å (1.27°)		0.013 Å (1.48°)	
B factors[e]/Å^2	8.6/10.0/9.4/21.5		16.3/18.8/36.5/33.1	
Residues	329		321	
Water molecules	586		395	
PDB ID	1ODM		1ODN	

[a] $R_{merge} = \Sigma_j\Sigma_h|I_{h,j} - \langle I_h\rangle|/\Sigma_j\Sigma_h\langle I_h\rangle \times 100$. [b] $R_{cryst} = \Sigma||F_{obs}| - |F_{calc}||/\Sigma|F_{obs}| \times 100$. [c] R_{free} = based on 4% of the total reflections. [d] RMS deviation from ideality for bonds (and angles). [e] Average *B* factors in order: main chain, side chain, substrate and solvent.

a small difference in the region of the vinyl group. ACvG is bound to the protein by electrostatic interactions involving its carboxylate groups: a salt bridge is formed between the aminoadipoyl carboxylate and Arg187, and the vinylglycine carboxylate is in position to hydrogen bond with Tyr189, Ser281 and to Arg279 *via* a water molecule. The cysteinyl thiolate of ACvG is a ligand at the active site iron atom, as are the protein side-chains of His214, Asp216 and His270. As in the ACV complex, there is a water ligand in the site *trans* to His214. However, in contrast to the complex with the natural substrate, there is also a second water ligand at the metal, in the site opposite Asp216, near the vinylglycine side-chain. In accommodating the extra water ligand at this site, the vinylic side-chain adopts a conformation which places the terminal CH_2 group in the pocket that is occupied by the *pro-R* methyl group in the IPNS:Fe(II):ACV complex (the methyl group further from iron). In this orientation, the vinyl group of ACvG is close to the oxygen binding site opposite Asp216, well placed for reaction with the proposed iron(IV)–oxo species.[2] However, the additional water ligand must presumably be displaced from iron before oxygen can bind to initiate the oxidative reaction.

Structure of the IPNS:Fe(II):HMPen complex

Crystals of IPNS:Fe(II):ACvG were exposed to high pressures of oxygen gas to initiate turnover in the active site. A crystal that had been exposed to 20 bar oxygen for 410 minutes allowed collection of a 1.60 Å resolution dataset, with active site electron density consistent with an IPNS:Fe(II):HMPen complex (Fig. 2b).

There are two key changes in the structure of the substrate-derived electron density from the IPNS:Fe(II):ACvG complex, and it is observation of these changes that form the basis for assigning the active site electron density as the HMPen molecule (the product observed when ACvG was incubated with IPNS in solution). Firstly, the cysteinyl sulfur atom has moved relative to the anaerobic structure: there is weaker electron density at the position it occupied in the anaerobic structure (which may correspond to residual ACvG or a low-occupancy water molecule) and a significant increase in electron density at a new position, further from the iron. It appears that the cysteinyl sulfur has moved towards the vinylglycine β-carbon, leaving its former binding site opposite His270 vacant. A similar migration of sulfur around iron was observed to have occurred in the IPNS:Fe(II):IPN complex.[3] These results are in contrast to turnover structures in which the reaction cycle has been intercepted before thiazolidine ring-closure. In the monocyclic β-lactam formed from δ-(L-α-aminoadipoyl)-L-cysteinyl-D-*S*-methylcysteine (ACmC), the cysteinyl sulfur atom occupies essentially the same position as it does in the starting IPNS:Fe(II):ACmC complex.[3] The same is also true of the cysteine-derived sulfur in the thiocarboxylic acid product arising from δ-(L-α-aminoadipoyl)-L-cysteine D-α-hydroxyisovaleryl ester (AC*O*V).[9] Movement of the cysteinyl sulfur atom therefore appears to be indicative of thiazolidine closure.

Connected to the movement of the cysteinyl sulfur, there is no electron density in the position that the cysteinyl β-carbon occupies in the anaerobic structure. This change, considered in combination with the changes to the sulfur-derived electron density discussed above, is consistent with movement of the cysteinyl β-carbon to a position much closer to the vinylglycine-derived nitrogen, in keeping with formation of a covalent bond between these two atoms.

Secondly, there is strong additional electron density adjacent to the region previously occupied by the vinylglycine side-chain. This is consistent with the presence of an extra oxygen atom in this region, and with appreciable movement of the vinylglycine CH_2 group having occurred. The model of the pendant hydroxymethyl chain fits well to the observed density. The stereochemistry of this group seems unequivocal, and consistent with the 2-α-hydroxymethylpenam product **4** observed in the solution studies.[5]

The average refined temperature factor (*B* factor) of the HMPen molecule is high compared to that of the protein (Table 1), which suggests lower occupancy of the HMPen product. However, in general the electron density is convincing and in keeping with the presence of HMPen, the product formed from the reaction in solution. Only for the β-lactam carbonyl and the thiazolidine sulfur is the electron density weak. The position of this carbonyl group suggests that it is similarly orientated to the equivalent carbonyls in both the IPNS:Fe(II):IPN structure and the structure of the monocyclic β-lactam generated from ACmC.[3] In all these cases, the carbonyl oxygen has moved relative to the starting complexes, rotating *ca.* 60° around the axis of the cysteinyl C_1–C_α bond towards Phe211, into the same plane as the atoms of the β-lactam ring. The poorer definition

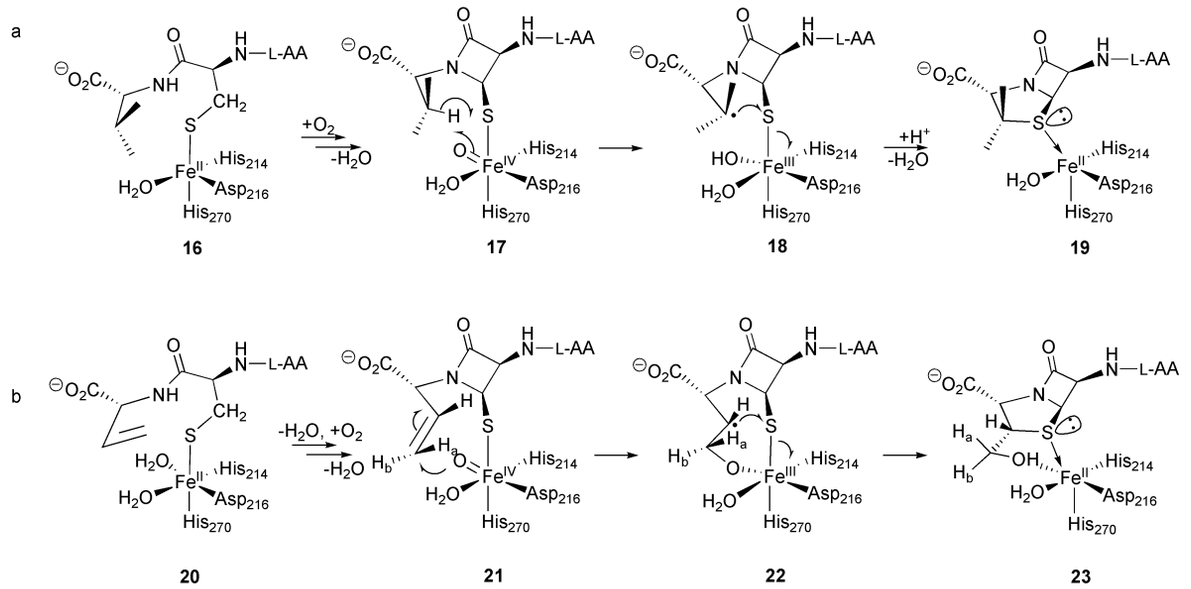

Fig. 3 **a**, Mechanism for the conversion of ACV **1** to IPN **2** by IPNS; **b**, the revised mechanism for conversion of ACvG **3** to HMPen **4** by IPNS. L-AA = L-α-aminoadipoyl.

of the carbonyl group in this case is consistent with the changing shape of the molecule overall; from an overlay of the ACvG and HMPen structures (Fig. 2c) it can be seen that the β-lactam carbonyl is the region in which greatest movement occurs in the conversion of ACvG to HMPen. Furthermore, without the tether provided by ligation of the cysteinyl thiolate to iron, a greater degree of freedom is imparted to this region of the molecule. It is interesting to note that the β-lactam carbonyl is also the least well defined region of the product in the electron density map of the IPNS:Fe(II):IPN complex.[3] Thus the original hypothesis that the α-hydroxymethyl group could aid the capture of a bicyclic penam by stabilising the IPNS:Fe(II):product complex through a bond to iron(II) is only partly validated, since the additional link is not in the region that undergoes greatest movement during substrate turnover.

Overall protein structure

The overall structure of the IPNS:Fe(II):HMPen complex corresponds closely to the unexposed IPNS:Fe(II):ACvG complex (RMS difference 0.202 Å). Interestingly however, there is little electron density corresponding to the eight residues at the protein C-terminus (Leu324–Thr331) in the product structure. Thus, it was concluded that these residues are disordered and this region was deleted from the model after the first round of refinement. On the basis of the previously published IPNS:Mn(II)[12] and IPNS:Fe(II):ACV[11] structures, it has been proposed that the substrate and the C-terminus compete as ligands for the iron binding site *trans* to His270. In the absence of substrate, the C-terminus enters the active site and Gln330 binds to the metal; upon substrate binding, Gln330 is displaced from iron and the eight C-terminal amino acids adopt a position over the active site entrance.[11] It follows that the C-terminus may become more mobile after the reaction is complete, to allow the product to leave the active site. The observed lack of discrete electron density for the C-terminus is consistent with mobility in this region of the protein, which could in turn be directly linked to substrate turnover having occurred in the crystal.

Connected to the mobility of the C-terminus, it has been noted previously that the side-chain of Phe211 occupies different conformations in the presence and absence of the natural substrate, undergoing a rotation of *ca.*120° about the C_α–C_β bond when ACV binds.[11] The conformation of this side-chain in the IPNS:Fe(II):ACvG complex mirrors that seen in the IPNS:Fe(II):ACV structure, while in the IPNS:Fe(II):HMPen complex Phe211 has rotated 120° to return to the orientation seen in the IPNS:Mn(II) structure. The conformation of the Phe211 side-chain in the unexposed enzyme:substrate complexes is such that it partially obscures the entrance to the active site. Thus rotation of this side-chain may be necessary in order to permit departure of the product once formed. It seems plausible that just as the eight C-terminal residues might move as part of the product release process, so too this rotation of Phe211 occurs upon formation of the product, and is linked to product departure from the active site.

There is a small amount of additional electron density visible in the IPNS:Fe(II):HMPen complex, in the space that is occupied by Phe211 in the unexposed complexes. This density appears to originate as a branch from the aminoadipoyl-cysteinyl peptide bond of the substrate, so it is possible that it arises from a small amount of the product on its way out of the active site. However it is equally possible that this density corresponds to several poorly ordered water molecules.

Mechanistic conclusions

In light of the results reported here and other structural information now available for IPNS,[3,11] as well as structural and spectroscopic information from other related oxygenase enzymes, it is possible to propose a revised mechanism for the IPNS reaction with ACvG (Fig. 3b). Rather than the [$2\pi_s + 2\pi$] cycloaddition proposed previously (Fig. 1b),[6,7] the iron(IV)–oxo moiety of intermediate **21** could instead instigate a single-electron reaction with the double bond. Attack on the less substituted end would give the secondary radical **22**, the more substituted of the two possible radical intermediates. This species closely resembles the radical intermediate **18** thought to be involved in the conversion of ACV to IPN. Attack of the radical in **22** on the cysteinyl sulfur, with concomitant homolysis of the S–Fe bond, would lead directly to formation of the HMPen complex **23**.

While the cycloaddition alternative cannot be discounted altogether, the radical mechanism is more in line with that believed to operate during thiazolidine closure in the reaction of IPNS with its natural substrate ACV (Fig. 3a). Furthermore, it avoids the need either to displace the second water ligand from iron, or to expand the metal's coordination sphere beyond six—one of these alternatives would be required for the cycloaddition mechanism, which leads to a metallocyclic intermediate incorporating three bonds from the tripeptide-derived species to iron. The radical mechanism is also consistent with the stereoselectivity seen in experiments with stereospecifically

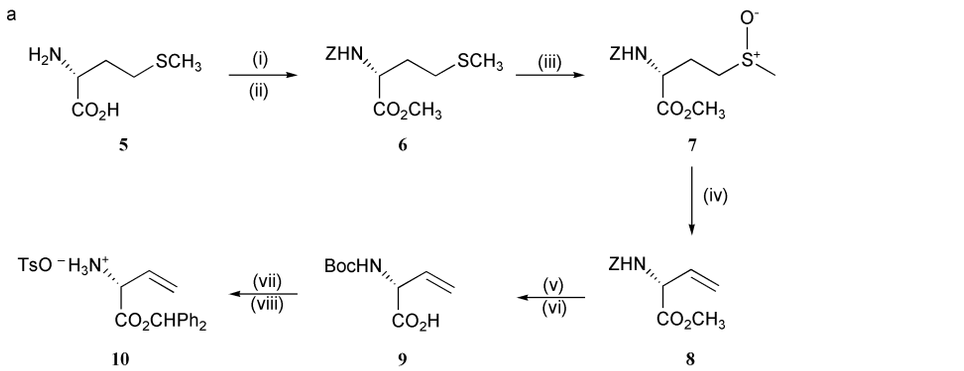

(i) $Me_2C(OMe)_2$, conc. HCl, rt, 36h, 82%; (ii) $PhCH_2OCOCl$, K_2CO_3, EtOAc/H_2O, 0°C to rt, 2h, 97%; (iii) $NaIO_4$, MeOH/H_2O, 0°C, 2h, 82%; (iv) 150°C, 0.5mmHg, 2h, 55%; (v) 3M HCl, reflux, 4.5h, 100%; (vi) $(BOC)_2O$, Et_3N, H_2O/1,4-dioxane, rt, 20 h, 84%; (vii) Ph_2CN_2, EtOAc, rt, 3.5h, 77%; (viii) TsOH, Et_2O/EtOH, -10 to 40°C, 100%.

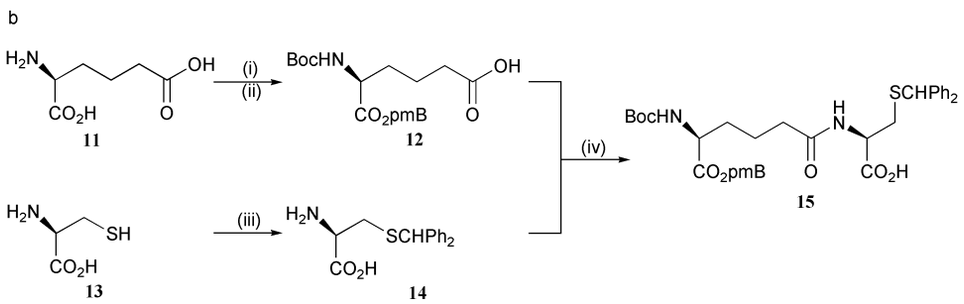

(i) $(BOC)_2O$, NaOH, H_2O/^{t}BuOH, rt, 48h, 98%; (ii) $MeOC_6H_4CH_2Cl$, Et_3N, DMF, 35°C, 24h, 53%; (iii) Ph_2CHOH, CF_3CO_2H, rt, 0.5h, 94%; (iv) **12**, ^{i}BuOCOCl, Et_3N, THF, -15°C, 0.5h, then **14**, Et_3N, H_2O, -15 to 0°C, 2h, 85%.

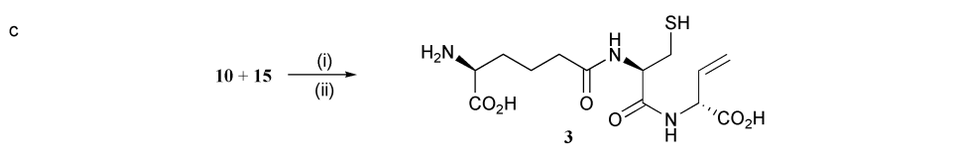

(i) EEDQ, Et_3N, Na_2SO_4, CH_2Cl_2, rt, 20h, 25%; (ii) CF_3CO_2H, $PhOCH_3$, reflux, 0.5h, then HPLC, 17%

Fig. 4 Synthesis of ACvG **3** from D-methionine **5**, L-α-aminoadipic acid **11** and L-cysteine **13**. L-AA = L-α-aminoadipoyl.

labelled ACvG isotopomers.[8] Since the radical intermediate **22** is tethered to iron through its pendant oxygen, free rotation is not possible and stereochemical integrity would be preserved.

The reaction of IPNS with ACvG in the crystalline state provides further structural information on the complexes of this enzyme with its bicyclic penam products. Moreover, these crystallographic studies allow revision of the previously proposed mechanism to better account for the structural information now available.

Experimental

Synthesis of the substrate analogue

D-Vinylglycine hydrochloride salt was prepared from *N*-Z-D-methionine methyl ester by periodate oxidation to the sulfoxide, flash vacuum pyrolysis and acid deprotection (Fig. 4a).[13] The amino acid was protected as its benzhydryl ester,[14] then converted to the fully protected tripeptide by standard methods (Figs. 4b, c).[15,16] Finally, acid-mediated deprotection afforded the tripeptide substrate analogue ACvG **3**.[17] The crude product was purified by reversed phase HPLC [ODS (250 × 10 mm), 10 mM NH_4HCO_3 in water–methanol as eluant (running time 0–5 minutes: 0% methanol; 5–12 minutes: gradient of 0–25% methanol; 13–18 minutes: 2.5% methanol; 18–20 minutes: 0% methanol v/v), 4 ml min^{-1}, λ = 254 nm, 5 AUFS (absorbance units full scale); t_r = 11 min].

Crystallisation and turnover experiments

Crystals of the IPNS:Fe(II):ACvG complex were grown anaerobically as previously,[18] although careful seeding allowed the growth of larger crystals than had previously been obtained (maximum dimensions 1.2 × 0.5 × 0.5 mm). For determination of the anaerobic IPNS:Fe(II):ACvG structure, crystals were flash-frozen in liquid nitrogen directly upon removal from the anaerobic environment. Crystals for oxygenation experiments were transferred to the pressurisation device on a glass cover slip and reaction was initiated at room temperature by exposure to dioxygen at 20 bar.[10] A range of pressurisation times was investigated, with the best result obtained after a 410 minute oxygenation. Following oxygen exposure the crystals were returned to atmospheric pressure and rapidly flash-frozen. The frozen crystals were stored under liquid nitrogen until required for data collection.

Data collection

Data were collected at 100 K using synchrotron radiation and an ADSC Quantum 4 detector at beamline ID14-EH4 of the European Synchrotron Radiation Facility, Grenoble, France (IPNS:Fe(II):ACvG structure), or a 300 mm Mar Research Image Plate at Station 7.2 of the Synchrotron Radiation Source, Daresbury, UK (IPNS:Fe(II):HMPen structure).

Structure determination

Data was processed using MOSFLM[19] and the CCP4 suite.[20] Refinement was carried out using REFMAC5.[21] The program O[22] was used for model building. Initial rigid body refinement was followed by refinement of all atoms and individual atomic temperature factors. Manual rebuilding of protein side-chains was performed as necessary.

For the IPNS:Fe(II):ACvG structure, electron density for the substrate ACvG was clearly visible throughout refinement. Data from the oxygenated crystal gave a structure with active site electron density consistent with high occupancy of a bicyclic penam molecule (HMPen), and possible occupancy of the unreacted substrate ACvG at a low level.

For the unexposed IPNS:Fe(II):ACvG structure, the initial refinements of positional and individual isotropic temperature factors were followed by refinement of individual anisotropic temperature factors when the model was complete. For the IPNS:Fe(II):HMPen structure, the final round of refinement included refinement of TLS parameters.[23] For the HMPen molecule, coordinate restraints were generated from selected analogous structures in the Cambridge Structural Database (CSD) of the Chemical Database Service (CDS).[24] Data collection and refinement statistics are given in Table 1.

Acknowledgements

We would like to thank the beamline scientists at the SRS Daresbury and the ESRF Grenoble for their assistance. This work was supported by the MRC, BBSRC and EPSRC, UK. P.J.R. was supported by the Rhodes Trust, N.I.B. by a German DAAD fellowship and P.L.R. by the Royal Society.

References

1 J. E. Baldwin and C. J. Schofield, in *The biosynthesis of β-lactams*, ed. M. I. Page, Blackie, Glasgow, 1992, p. 1–78.
2 J. E. Baldwin, *Spec. Publ. - R. Soc. Chem.*, 1985, **52**, 62–85.
3 N. I. Burzlaff, P. J. Rutledge, I. J. Clifton, C. M. H. Hensgens, M. Pickford, R. M. Adlington, P. L. Roach and J. E. Baldwin, *Nature*, 1999, **401**, 721–724.
4 J. E. Baldwin and M. Bradley, *Chem. Rev.*, 1990, **90**, 1079–1088.
5 J. E. Baldwin, R. M. Adlington, A. Basak, S. L. Flitsch, A. K. Forrest and H.-H. Ting, *J. Chem. Soc., Chem. Commun.*, 1986, 273–275.
6 J. E. Baldwin, R. M. Adlington, S. L. Flitsch, H.-H. Ting and N. J. Turner, *J. Chem. Soc., Chem. Commun.*, 1986, 1305–1308.
7 J. E. Baldwin, R. M. Adlington, L. G. King, M. F. Parisi, W. J. Sobey, J. D. Sutherland and H.-H. Ting, *J. Chem. Soc., Chem. Commun.*, 1988, 1635–1637.
8 S. D. Abbott, 1991, D Phil Thesis, University of Oxford.
9 J. M. Ogle, I. J. Clifton, P. J. Rutledge, J. M. Elkins, N. I. Burzlaff, R. M. Adlington, P. L. Roach and J. E. Baldwin, *Chem. Biol.*, 2001, **8**, 1231–1237.
10 P. J. Rutledge, N. I. Burzlaff, J. M. Elkins, M. Pickford, J. E. Baldwin and P. L. Roach, *Anal. Biochem.*, 2002, **308**, 265–268.
11 P. L. Roach, I. J. Clifton, C. M. H. Hensgens, N. Shibata, C. J. Schofield, J. Hajdu and J. E. Baldwin, *Nature*, 1997, **387**, 827–830.
12 P. L. Roach, I. J. Clifton, V. Fülöp, K. Harlos, G. J. Barton, J. Hajdu, I. Andersson, C. J. Schofield and J. E. Baldwin, *Nature*, 1995, **375**, 700–704.
13 D. H. Rich and J. P. Tam, *J. Org. Chem.*, 1977, **42**, 3815–3820.
14 S. Wolfe and M. G. Jokinen, *Can. J. Chem*, 1977, **57**, 1388–1396.
15 J. E. Baldwin, S. R. Herchen, B. L. Johnson, M. Jung, J. J. Usher and T. Wan, *J. Chem. Soc., Perkin Trans. 1*, 1981, 2253–2257.
16 J. C. Sheehan, J. Preston and P. A. Cruickshank, *J. Am. Chem. Soc.*, 1965, **87**, 2492–2493.
17 M. Bodanzky and A. Bodanzky, in *The practice of peptide synthesis*, ed. K. Hafner, C. W. Rees, B. M. Trost, J. M. Lehn, R. v. R. Schleyer and R. Zahruchik, Springer-Verlag, Berlin, 1984, p. 172.
18 P. L. Roach, I. J. Clifton, C. M. H. Hensgens, N. Shibata, A. J. Long, R. W. Strange, S. S. Hasnain, C. J. Schofield, J. E. Baldwin and J. Hajdu, *Eur. J. Biochem.*, 1996, **242**, 736–740.
19 A. G. W. Leslie, *Acta Crystallogr., Sect D*, 1999, **55**, 1696–1702.
20 Collaborative Computational Project Number 4, *Acta Crystallogr., Sect. D*, 1994, **50**, 760–763.
21 G. N. Murshudov, A. A. Vagin, A. Lebedev, K. S. Wilson and E. J. Dodson, *Acta Crystallogr., Sect. D*, 1999, **55**, 247–255.
22 T. A. Jones, J. Y. Zou, S. W. Cowan and M. Kjeldgaard, *Acta Crystallogr., Sect. A*, 1991, **47**, 110–119.
23 M. D. Winn, M. N. Isupov and G. N. Murshudov, *Acta Crystallogr., Sect. D*, 2001, **57**, 122–133.
24 D. A. Fletcher, R. F. McMeeking and D. Parkin, *J. Chem. Inf. Comput. Sci.*, 1996, **36**, 746–749.